A R C H I V E S O F M E T A L L U R G Y A N D M A T E R I A L S
Volume 58 2013 Issue 2
DOI: 10.2478/amm-2013-0032

Ł. KACZMAREK*, M. STEGLIŃSKI*, J. SAWICKI*, J. ŚWINIARSKI**, D. BATORY*, K. KYZIOŁ***, Ł. KOŁODZIEJCZYK*, W. SZYMAŃSKI*, P. ZAWADZKI*, D. KOTTFER****

OPTIMIZATION OF THE HEAT TREATMENT AND TRIBOLOGICAL PROPERTIES OF 2024 AND 7075 ALUMINIUM ALLOYS

OPTYMALIZA OBRÓBKI CIEPLNEJ I WŁAŚCIWOŚCI TRIBOLOGICZNYCH STOPÓW ALUMINIUM 2024 I 7075

This paper describes two stages of optimization of the properties of 2024 and 7075 aluminium alloys, in particular their resistance to pitting by first T6, T6I6 or T6I4 treatment, and second increase its tribological properties by depositing by RF PACVD method a gradient coating of high adhesion to the substrate.

Quantitative microstructural characteristics reveals that it is possible to increase hardness (up to 190HV for 7075 alloy) with relatively high yield strength (520 MPa) and high ultimate elongation (about 20%) by optimizing dispersion of precipitates using two-stage artificial aging process.

Next to eliminate forming of thin Al_2O_3 layer with relatively poor adhesion to the aluminium substrate, gradient a-C: H/Ti layers synthesis hybrid plasma chemical RF PACVD reactor equipped with pulsed magnetron sputtering system was used. Using such configuration enables forming a thick and highly adherent diamond-like carbon layer on aluminium surface with low coefficient of friction (0.05), at a substrate temperature below 470K. Due to application of Ti magnetron cathode it was possible to improve the adhesion strength up to 30mN of diamond-like carbon layer to the covered substrate. Influence of deposition parameters on microhardness profile as well as adhesion and morphology were determined by nanotest and AFM, respectively.

Keywords: aluminium alloy, heat treatment, coating, coefficient of friction

W niniejszym artykule przedstawiono wyniki badań doboru parametrów dwuetapowego procesu obróbki cieplnej stopów aluminium, w szczególności podwyższenia odporności na pitting poprzez zastosowanie obróbki T6, T6I4 lub T6I6 oraz odporności na zacieranie poprzez osadzenie metodą RF PACVD warstw gradientowych o wysokiej adhezji do podłoża.

Przeprowadzona analiza wyników badań dowodzi, że istnieje możliwość podwyższenia twardości (nawet do 190 HV dla stopu 7075) przy relatywnie wysokiej jego granicy plastyczności (520 MPa) i wysokim wydłużeniu przy zerwaniu (20%) na drodze optymalizacji dyspersji wydzieleń poprzez zastosowanie dwuetapowego starzenia.

W celu wyeliminowania tworzenia się cienkiej warstwy Al_2O_3 charakteryzującej się relatywnie niska adhezją do podłoża osadzono, przy pomocy reaktora RF PACVD wyposażonego w źródło rozpylania magnetronowego, gradientową powłokę a-C: H/Ti. Zastosowanie niniejszej konfiguracji umożliwiło w temperaturze poniżej 470K wytworzenie na podłożu aluminiowym cienkiej, dobrze przylegającej powłoki węglowej charakteryzującej się niskim współczynnikiem tarcia (0.05). Zastosowanie tytanowej katody magnetronowej umożliwiło osiągnięcie wartości adhezji powłoki węglowej do podłoża na poziomie 30 mN.

Wpływ parametrów osadzania zarówno na profil mikrotwardości jak i adhezję oraz morfologię przebadano przy użyciu technik nanoindentacji oraz Mikroskopu Sił Atomowych.

1. Introduction

The vast growth of applications range of aluminium alloys is bound up with the search for alternative materials reducing the total construction weight as well as its maintenance cost and lowering greenhouse effect. The prospective area where aluminium alloys may be used is armaments industry e.g. in the production of unmanned aerial vehicles, transport or spy robots. Apart from aviation and armaments industry, aluminium alloys become widely used in automotive industry (sport and racing cars) as well as in medicine, where Al alloys are experimentally used in surgeon robots [1-5].

Studies conducted by Williams & Starke [6], Funatani [7], Salazar-Guapuriche [8], Warner [9], Leśniak [10, 11] or Richert [12] during the last ten years have proved that aluminium alloys, which might be used in elements exposed to high level of stress and wear are the ones intended for plastic forming: series 2xxx (with Cu), series 7xxx (with Zn) and series 8xxx (with Li). Alloys of series 2xxx and 7xxx called duralumin are characterized by exceptional properties such as:

* INSTITUTE OF MATERIAL SCIENCE AND ENGINEERING, TECHNICAL UNIVERSITY OF ŁÓDŹ, UL. STEFANOWSKIEGO 1/15, 90-924 ŁÓDŹ, POLAND
** TECHNICAL UNIVERSITY OF LODZ, DEPARTMENT OF STRENGTH OF MATERIALS AND STRUCTURES, STEFANOWSKIEGO 1/15, 90-924 ŁÓDŹ, POLAND
*** FACULTY OF MATERIALS SCIENCE AND CERAMICS, AGH UNIVERSITY OF SCIENCE AND TECHNOLOGY, AL. MICKIEWICZA 30, 30-059 KRAKÓW, POLAND
**** DEPARTMENT OF TECHNOLOGIES AND MATERIALS, FACULTY OF MECHANICAL ENGINEERING, TECHNICAL UNIVERSITY IN KOŠICE, MÄSIARSKA 74, 040 01 KOŠICE

high specific strength, high resistance to stress corrosion cracking as well as high resistance to brittle fracture. This is the case where improvement of resistance to contact fatigue is realized by optimization of heat treatment parameters by precipitate hardening of one- and two-stage treatment of artificial aging of multi-component aluminium alloys [1-4]. However, for improvement of resistance of aluminium alloys to abrasive wear the most commonly used methods of coating deposition are: physical vapour deposition – (PVD), plasma assisted chemical vapour deposition – (PACVD) [13,14], magnetron sputtering, ion implantation [15], pulsed laser deposition – (PLD) [16-20], in fluidized bed [21] and thermal spraying [22,23]. Nevertheless, only several of these methods seem to be applicable due to relatively high parameters of deposition of protective coatings. The limited application is caused by sensitivity of aluminium alloy structure in temperatures above 470K. Exceeding this temperature may result in grain growth and precipitates coagulation, what may lead to deterioration of mechanical properties of base material. From the above methods of coating deposition the RF PACVD [24,25] seems to be a feasible method to be used for large scale commercial production.

2. Experimental details

In this study two aluminium alloys 2024 and 7075 were used, which are multi-component alloys intended for precipitation hardening realized by heat treatment.

During the first stage of this study the temperature and time needed for each of the types of heat treatment used were specified (see Table 1). In order to define the influence of the type of heat treatment on the quantity, size and dispersion of emerging hardening phases in continuum, test pieces were put under microscopic observation and visually analyzed using Met-Ilo v.5.1. software. Moreover static tension test was conducted on universal strength testing machine INSTRON 4485 in order to confirm heat treatment parameters influence on resistance to cracking of the studied aluminium alloys.

During the second stage of this study Ti/TiC/a:CH gradient coatings, using hybrid plasma chemical RF PACVD reactor equipped with impulse magnetron sputtering, were deposited. Thanks to this it was possible to deposit carbon coating of high adhesion to various base materials. The widely discussed in international literature problem of internal stresses and relatively low adhesion was solved by using a thin Ti interlayer of 100nm thickness. The chemical constitution in gradient coating varies from pure Ti directly on the base material to thick carbon layer on the coating surface. The use of magnetron cathode enabled an increase of carbon layer adhesion to the base material. In addition, titanium carbides which may occur in the matrix of amorphous carbon ensure smooth uniform connection between the two phases appearing in the layer structure during deposition. Thanks to the new technology used for the synthesis the coating with low friction coefficient, high hardness, wear resistance, good biological and corrosion properties was obtained [26].

Next, mechanical properties of deposited coatings were investigated. The nanoscratch and hardness distribution test were carried out with a Nanoindenter G200 (MTS System, USA) using a diamond conical indenter with included angle of 90deg and Berkovich indenter, respectively. The friction coefficient was examined with pin-on-disk method using T-11 Tribotester under following conditions: track length – 500m, load – 5N, rotational speed – 95rpm, linear velocity 0,1m/s. The morphology analysis of deposited coating was conducted using atomic force microscope (AFM) „Metrology Series 2000" (Molecular Imaging, USA).

TABLE 1

Substrate	Type of tempers	Time and temperature of solid solution treatment	Time and temperature of ageing treatment	
2024	T6	773K 6h	353K or 393K or 433K - 12h	
	T6I6		**1st stage**	**2nd stage**
			393K 1,5h	353K or 393K or 433K - 12h
	T6I4		**1st stage**	**2nd stage**
			393 1h	297K or 338 - 12h
7075	T6	813K 6h	353K or 393K or 433K - 12h	
	T6I6		**1st stage**	**2nd stage**
			393K 1,5h	353K or 393K or 433K - 12h
	T6I4		**1st stage**	**2nd stage**
			393K 1h	297K or 338 - 12h

During the last stage of the study, the computer simulation was conducted to check the behavior of the created material with coatings in the real work conditions. Numerical simulations were performed using ANSYS application for real gear wheel with small module pitch working in military spy-robot. Discrete model (Figure 10a) was built and loaded according to the real technical data of the gear wheels.

3. Experimental results

3.1. Heat treatment of aluminium alloys

The analysis of hardness evolution (Figure 2, 4) and specific resistance (Figure 1, 3) of 2024 and 7075 alloys during ageing process (T6) shows that the most dynamic change of these properties occurred during the first 90 minutes. After that time specific resistance reached its minimum whereas hardness reached its maximum (150 and 168 $HV_{0,1}$, respectively) at ageing temperature of 433K. In the case of T6I6 and T6I4 treatment, the analysis of same properties for both alloys proves that the most significant changes occurred during the first segment of ageing (60 minutes). However, during the second segment of ageing these properties changed dynamically, in particular during the first 10 to 20 minutes, which resulted in obtaining the maximum hardness of 160 $HV_{0,1}$ for 2024 alloy (for both T6I4 and T6I6 treatment) as well as for 7075 alloy with maximum hardness of 170 $HV_{0,1}$ and 186 $HV_{0,1}$ (for T6I4 and T6I6, respectively).

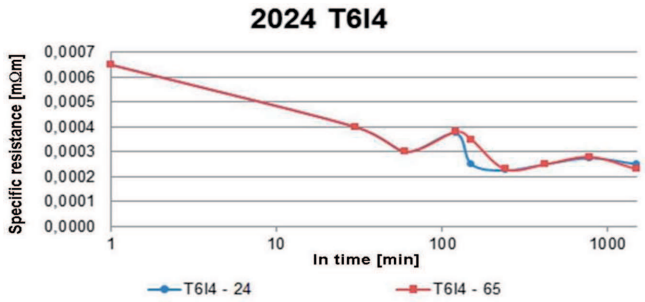

Fig. 1. Kinetics of specific resistance for 2024 alloy during T6I4 treatment

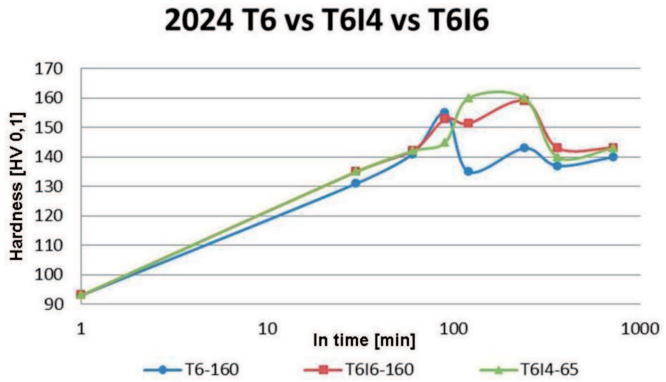

Fig. 2. Comparison of kinetics of hardness increase for 2024 alloy respectively aged using: T6, T6I4 and T6I6 treatment

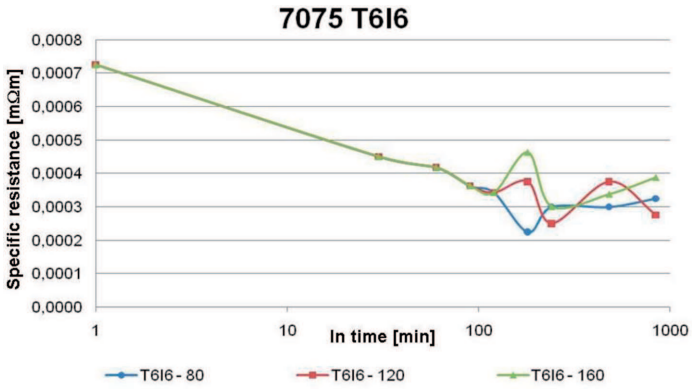

Fig. 3. Kinetics of specific resistance for 7075 alloy during T6I4 treatment

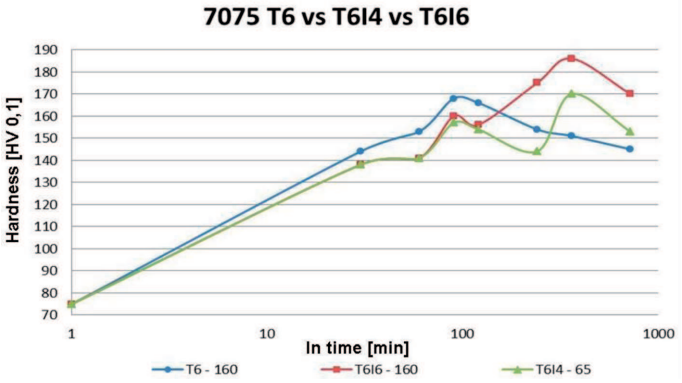

Fig. 4. Comparison of kinetics of hardness increase for 7075 alloy respectively aged using: T6, T6I4 and T6I6 treatment

3.2. Morphological and Mechanical analysis of heat treated aluminium alloys

The morphology observation of 2024 and 7075 alloys proved that application of two-stage ageing (T6I4, T6I6) causes small precipitates formation of significant quantity. It leads to the improvement of mechanical properties, particularly hardness (Figure 5). Furthermore, it was observed that during one-stage ageing (T6) the emerging phases were precipitated to a lesser extent and they were larger in size in comparison to those emerging while two-stage treatment. Large infrequently distributed precipitates make strengthening of the alloy insignificant, due to the fact that large phases do not constitute sufficiently large obstacles for dislocation movement.

The results of the tensile test confirmed the influence of selected heat treatment parameters on such material properties as yield strength, resistance to cracking and maximum strain when fracture occurred. In the case of supersaturated 2024 alloy the yield strength was 250MPa, whereas maximum strain at the moment of fracture was at 48% level. The best strength parameters were obtained after T6I6 treatment, where the yield strength was 300MPa and maximum strain at the moment of fracture was at 42% level. Similar properties were obtained after T6I4 treatment, 299MPa and 36%, respectively. Comparing these values with these of T6 treatment (289MPa and 33%) it can be claimed that two-stage ageing process results in a significant increase of resistance to cracking (from 33% to 42%) and strengthening of 2024 alloy.

Analyzing the tensile test results of supersaturated 7075 alloy, yield strength and maximum strain when fracture occurred equal 253MPa and 33% respectively. The best strength properties were obtained after T6I4 treatment, where $R_{0,2}$ was 460MPa and strain at fracture point was 31%. The results after T6 and T6I6 treatments are very similar. For single-stage ageing yield strength $R_{0,2}$ reached 560MPa, while maximum strain when fracture occurred was 24%. After the multi-stage treatment T6I6 $R_{0,2}$ reached 520MPa and strain was 22%. In case of T6I4 $R_{0,2}$ was 460MPa and strain was 31%. Therefore, it may be concluded that in case of 7075 alloy the two-stage treatment leads to an increase of resistance to cracking (21% to 31%), similarly as for 2024 alloy.

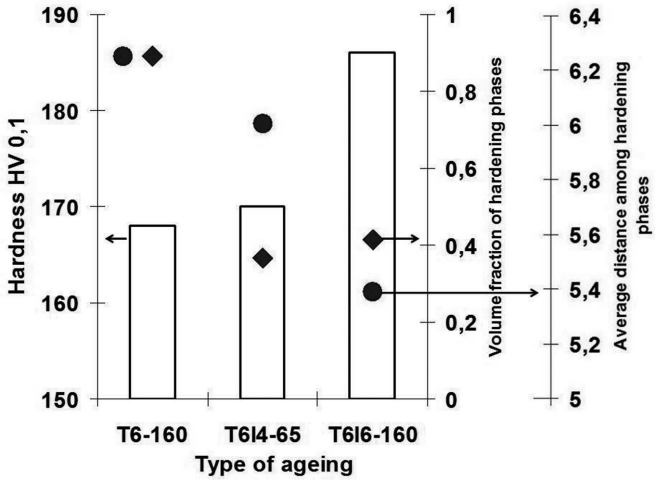

Fig. 5. An example of influence of ageing condition on volume frac-

tion of hardening phases and average distance among hardening phases on hardness for 7075 alloy

3.3. Ageing of aluminium alloys while coating deposition

Taking into account the results above, samples of 2024 and 7075 alloy were supersaturated and aged (only the first segment) according to experimentally determined parameters of heat treatment T6I4 and T6I6. The second segment of ageing was realized simultaneously while gradient Ti/TiC/a:CH coating deposition.

Analysis of the coating surface morphology confirms influence of substrate polarization on the size of emerging carbon domains. This is probably the consequence of the fact that during coating deposition with the substrate polarization the average kinetic energy of ionized carbon atoms increases. Higher kinetic energy lead to an increase of probability of knocking out carbon atoms already forming the coating. Carbon atoms knocked out from the coating surface create more spots with higher energy. These spots constitute crystallization nuclei for further carbon atoms. This is related to the observed decrease in the size of grains emerging on the sample surface when polarization increases, as shown in the Figure 6.

Nanoindentation testing proved that hardness and modulus are proportional to substrate polarization value. The higher the polarization, the better hardness and modulus of the coating were obtained (see Figure 7). In addition, during coating deposition precipitatation process took place in the substrate material increasing its hardness. The adhesion of deposited coatings to the substrate material is 30mN.

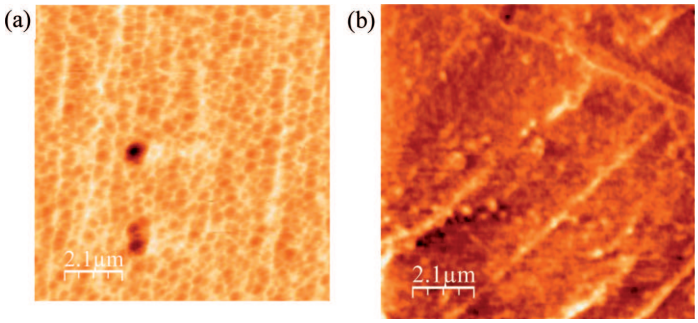

Fig. 6. Example pictures AFM of Ti/TiC/a:CH coatings respectively: (a) polarization of base during deposition – 150V, hardness of coating 10 GPa, (b) polarization of base during deposition – 600V hardness of coating 19 GPa

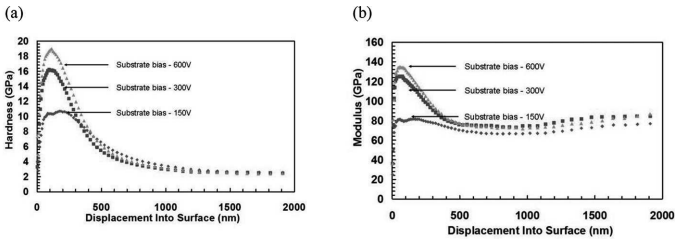

Fig. 7. Nanohardness profile (a) and longitudinal elastic modulus (b) Ti/TiC/a:CH coatings deposited using RF PACVD method for various base polarizations values

Friction coefficient testing of the coating shows that the one with the lowest hardness (10 GPa) had the best wear resistance. During the test the coating carries stresses, undergoes slow wear and due to its relatively low hardness becomes solid lubricant. The lowest value of friction coefficient (COF) was obtained for alumina counter-body (average value of 0.05) while the highest COF was measured for 52100 steel counter-body. In the case of coating with hardness of 19GPa the measured COF was 0.15 (steel counterbody). However, after about 2000 seconds the coating was destroyed and the friction coefficient increased rapidly up to 0.4. This phenomenon might be attributed to relatively high chemical affinity of the Fe atoms from counter-body to the carbon atoms of the coating. This causes rapid coating degradation during which hard products of coating delamination do not form solid lubricant as for the coating of 10GPa hardness. Instead, they act as the abrasives accelerating wear processes. In the case of both coatings of hardness 10GPa and 19GPa degradation processes in contact with Al_2O_3 counter-body were not observed (Figures 8 and 9). Counter specimen made of Al_2O_3 due to its relatively high bond energy and low chemical affinity to carbon atoms of the coating does not influence the initiation of degradation processes.

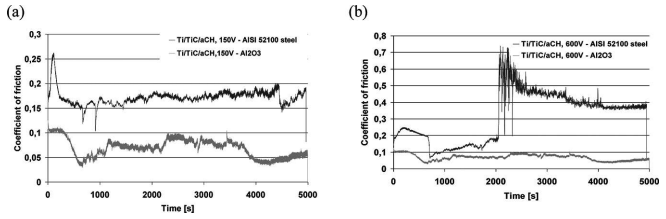

Fig. 8. Analysis of friction coefficient of coating Ti/TiC/a:CH deposited respectively with polarization of base (a) 150V and (b) 600V in contact with counter specimen: steel – AISC 52100 and Al_2O_3

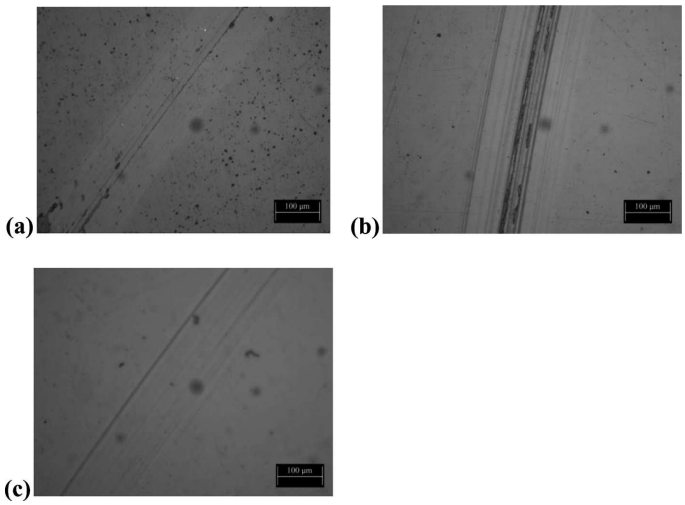

Fig. 9. Example view of wear lines of Ti/TiC/a:CH coatings deposited respectively with polarization of base (a) 150V, (b) 600V in contact with counter specimen Al_2O_3 and (c) 600V in contact with counter specimen – AISC 52100

3.4. Numerical simulations

To check the behavior of the created material with coatings in the real work conditions numerical simulations were performed. From the computer simulation for the wheel tooth

of real gear wheel with small module pitch working in military spy-robot, several stress distributions were obtained: reduced σ_{red} (Figure 10b), longitudinal σ_Y (Fig. 10c), transverse σ_X (Fig. 10d) and the position of Bielayev point Z_B. From the obtained longitudinal stress distribution σ_Y which results from external forces (Figure 10c) for 2024 (T6I6) alloy with Ti/TiC/a:CH coating it can be seen that on the side surface of the tooth mainly tension of about +116MPa occured. Compression occurs only around contact points of tooth with maximum of -600MPa. The value of reduced stress was about 451MPa and it was below yield strength of analyzed material. Deposited coating was not causing stress concentration on wheel surface because of little difference between coefficients of direct elasticity of coating and substrate material. Similar values of stress (difference about 5%) were obtained for wheel made of 7075 alloy after T616 treatment with Ti/TiC/a:CH coating. Computer simulation confirmed that proposed gradient coated alloys can be used for intended highly loaded elements, thus fulfilling the requirements of real exploitation conditions.

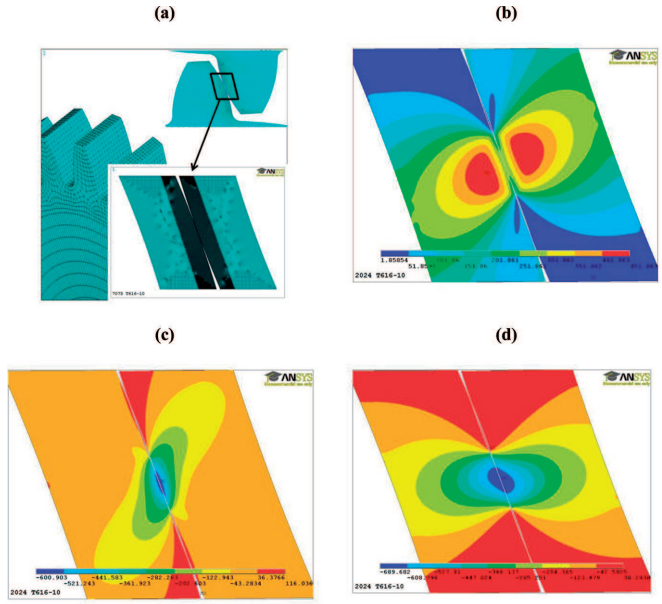

Fig. 10. Discrete model of friction node of gear wheels and selected submodel in the contact point of gear wheels (a), map of stress distribution: reduced (b), longitudinal (c), transverse (d)

4. Conclusions

The following conclusions may be formulated on the basis of the study results:

- In case of heat treatment of 2024 and 7075 alloy it is possible to increase hardness using two-stage aging (T6I6) by about 6% and 11%, respectively, in comparison to one-stage treatment (T6).
- It is possible to deposit gradient coatings on aluminium alloys with relatively high adhesion simultaneously with conducting precipitation processes in the substrate material.
- Deposited Ti/TiC/a:CH gradient coatings are characterized by high wear resistance and low friction coefficient at 0.05.
- Discussion presented in this paper is a compilation of results of theoretical, model and experimental studies which were partly independent of each other. Gathering the results together the thesis stated in introduction about utilitarian significance of analyzed aluminium alloys can be confirmed.

Acknowledgements

This work was supported by a grant of the Rector's Fund, Technical University of Lodz, Poland.

REFERENCES

[1] R.N. Lumley, J. Buha, I.J. Polmear, A.J. Morton, A.G. Crosky, Mat. Sci. Forum **519-521**, 283-290 (2006).
[2] R.N. Lumley, I.J. Polmear, A.J. Morton, International Patent Application PCT/AU02/00234 (2002).
[3] R.J. Rioja, Materials Science and Engineering **A257**, 100-107 (1998).
[4] R.N. Lumley, C. South, I.J. Polmer, M.A. North, A.J. Morton, United States Patent Application 20030041934 (2003).
[5] P. Uliasz, T. Knych, A. Mamala, Archives of Metallurgy and Materials **54**, 711-721 (2009).
[6] J.C. Williams, E.A. Starke, Acta Materialia **51**, 5775-5799 (2003).
[7] Funatani K La Metallurgia Italiana **2**, 67-73 (2006).
[8] M.A. Salazar-Guapuriche, Y.Y. Zhao, Mater. Sci. Forum **519-521** 853-858 (2006).
[9] T. Warner, Mater. Sci. Forum **519-521**, 1271-1278 (2006).
[10] D. Leśniak, M. Bronicki, A. Woźnicki, Archives of Metallurgy and Materials **55**, 449-513 (2010).
[11] D. Leśniak, Archives of Metallurgy and Materials **54**, 1135-1144 (2009).
[12] M. Richert, J. Richert, J. Zasadziński, S. Hawryłkiewicz, J. Długopolski, Mater. Chem. Phys. **81**, 528-530 (2003).
[13] B. Adamczyk-Cieślak, J. Mizera, M. Lewandowska, K.J. Kurzydłowski, Rev. Adv. Mater. Sci. **8**, 107-110 (2004).
[14] D. Batory, M. Cłapa, S. Mitura, Inżynieria Materiałowa **5**, 868-870 (2006).
[15] S. Gredelj, S. Kumar, A.R. Gerson, P. Cavallaro, Thin Solid Films **515**, 1480-1485 (2006).
[16] D. Manowa, S. Mandl, B. Rauschenbach, Surf. and Coat. Tech. **180-181**, 118-121 (2004).
[17] A.L. Thomann, E. Sicard, C. Boulmer-Leborgne, C. Vivien, J. Hermann, C. Andreazza-Vignolle, P. Andreazza, C. Meneau, Surf. and Coat. Tech. **97**, 448-452 (1997).
[18] B. Major, Archives of Metallurgy and Materials **50**, 35-46 (2005).
[19] M. Klimczak, A. Kopia, R. Chmielowski, J. Kusinski, I. Suliga, Mater. Chem. Phys. **81**, 558-561 (2003).
[20] R. Chmielowski, S. Villain, A. Kopia, J.P. Dallas, J. Kusinski, J.R. Gavarri, Ch. Leroux, Thin Solid Films **516**, 3747-3754 (2008).
[21] E. Sicard, C. Boulmer-Leborgne, T. Sauvage, App. Surf. Sci. **127-129**, 726-730 (1998).
[22] M. Okumiya, Y. Tsunekawa, T. Murayama, Surf. and Coat. Tech. **142-144**, 235-240 (2001).

[23] M. Wenzelburger, D. Lopez, R. Gadow, Surf. and Coat. Tech. **201**, 1995-200 (2001).
[24] B.B. Verma, J.D. Atkinson, M. Kumar, Bull. Mater. Sci. **24**, 231-236 (2001).
[25] A. Góral, J. Deda, E. Bełtowska-Lehman, B. Major, Archives of Metallurgy and Materials **53**, 979-984 (2008).
[26] M. Cłapa, D. Batory, Journal of Achievements in Materials and Manufacturing Engineering **20**, 415-418 (2007).

Received: 20 September 2012.